Enhancing CO_2 conversion with gas quenching in arc plasma

Rani Vertongen[1], Ivan Tsonev,[1] and Annemie Bogaerts[1]

[1] Research group PLASMANT, Department of Chemistry, University of Antwerp, Universiteitsplein 1, 2610 Antwerp, Belgium.

Corresponding author: Rani Vertongen, rani.vertongen@uantwerpen.be

Abstract

We investigated post-plasma gas quenching in an arc plasma for CO_2 conversion. We present experiments with a basic pin reactor, along with four different methods for quick cooling, i.e., a nozzle, wall cooling, combining the nozzle and wall cooling, and a heat exchanger. We demonstrate that quenching can significantly improve the performance. The best results are obtained with a heat exchanger, enhancing the conversion with a factor three (from 6 to above 18 %) and the energy efficiency with a factor 1.5 (from 20 to 30 %) when compared to the benchmark. Temperature measurements indeed confirm that the heat exchanger provides the most effective cooling. In addition, the heat exchanger ensures a more stable and elongated plasma which further improves the performance. Interestingly, we observe a linear increase between conversion and specific energy input, resulting in a constant energy efficiency of about 30 %, which is very promising for further upscaling towards higher specific energy input.

Keywords

Plasma; CO_2 conversion; arc; quenching; reactor design

Highlights

- Significant improvement of CO_2 conversion with post-plasma gas quenching.
- Heat exchanger results in three times higher conversion (from 6 to above 18 %) than the benchmark.
- Quenching ensures a constant energy efficiency of 30 % in the full SEI range.
- Stable plasma in takeover mode can elongate the arc and improve performance.
- MW and arc plasma demonstrate the same performance under similar conditions.

1. Introduction

Global warming is a complex problem and the pressure for change is high. Our greenhouse gas emission must be greatly reduced, preferably to net zero, to limit the worst consequences of climate change [1]. Direct electrification of industrial processes and innovative carbon capture and utilization are important strategies to pursue [2]. Among the novel electrified technologies such as electrochemistry, plasma reactors are gaining increasing interest for various applications, such as nitrogen fixation for fertilizer synthesis and CO_2 conversion into value-added products [3–6]. Especially so-called warm plasmas are promising, because of their better energy efficiency than cold plasmas. Indeed, stable molecules like CO_2 are easily decomposed by the high temperature (order of several 1000 K) characteristic for these plasmas [3,5]. Plasma reactors also have the advantage of instant process control with immediate production, thus coupling very well with fluctuating renewable electricity, and they do not rely on rare metal catalysts for good performance [6].

Arc plasma reactors are interesting for CO_2 conversion, thanks to their operation at atmospheric pressure [7]. They are characterized by relatively high gas temperatures, typically higher than 3000 K, enabling fast thermal reactions [3]. An important benefit is their flexible design and easy ignition, since no coupling to electromagnetic waves is needed to sustain the arc, as is the case for microwave (MW) discharges. However, our previous research has indicated that the conversion in such arc reactors, including gliding arcs, is limited to typically 10 % for a maximum energy efficiency of 30 % [8].

One of the most promising strategies for performance improvement is gas quenching, either to enhance the conversion or to tune the selectivity in plasmas operating (near) thermal equilibrium, e.g. in the production of acetylene from CH_4 plasma [9], and in CO_2 conversion [10]. By quickly cooling the plasma afterglow, the temperature drops fast enough to protect the products from reverse reactions in the effluent, e.g., for CO_2 conversion:

$$\mathrm{O} + \mathrm{CO} + \mathrm{M} \rightleftharpoons \mathrm{CO_2} + \mathrm{M} \tag{R1}$$

$$\mathrm{CO} + \mathrm{O_2} \rightleftharpoons \mathrm{CO_2} + \mathrm{O} \tag{R2}$$

The stable products are preserved in the case of ideal quenching, while reactive atoms and radicals are converted back into the initial reagents during cooling. In the case of super-ideal quenching, additional conversion occurs during the cooling process, when the atoms and radicals would react with the feed gas, converting it further into the products (i.e., the equilibrium of R2 shifts to the left) [11,12].

Several different experimental design principles have been applied already for quick cooling in CO_2 plasma reactors. For example, gas mixing by injecting cold gas in the hot stream can ensure high cooling rates. Chekmarev et al. applied counterflow quenching with the cooled gas from the reactor, leading to a factor four increase in CO_2 conversion (from 6 to 24 %), and four times increase in energy efficiency (from 5 to 20 %) [13]. Placing a nozzle constriction at the outlet can have a similar effect as gas mixing, since it increases the turbulence after the plasma, thereby mixing the hot core with the colder surrounding gas and improving heat loss to the walls [14,15]. Hecimovic et al. applied a cooled nozzle to a MW discharge, with significant improvements at 900 mbar and low CO_2 flow rates. Their CO_2 conversion increased with a factor seven (from 5 to 35 %) and the energy efficiency with a factor four (from 5 to 20 %) [15]. Mercer et al. obtained the largest relative increase in performance at a pressure of 300 mbar, with almost three times higher conversion when applying the converging-diverging nozzle (from about 10 to 30 %) and three times higher energy efficiency (from 8 to 23 %). At a higher pressure of 700 mbar, however, the improvement was only a factor 1.2 for both conversion and energy efficiency [16]. Li et al. combined a contracting nozzle with an argon arc plasma with CO_2 addition.

They observed an increase in effective conversion (from 2.4 to 22 %), i.e. a factor nine higher with the nozzle, and a parallel improvement in energy efficiency up to 18 % [17]. Some experiments at lower pressure with nozzles additionally aim for supersonic gas expansion in the effluent, as an alternative way to boost the cooling by converting the thermal energy into directional kinetic energy [15,18].

Cooling by direct contact with a cold wall can also improve the performance, for example by a surrounding double wall [19], a cooling rod in the center of the afterglow [20], or in multiple cooled outlet channels, similar to shell-and-tube heat exchangers [21,22]. Some of the best results to date were achieved by Hecimovic et al. in a MW discharge at atmospheric pressure with a heat exchanger (i.e., four cooled effluent channels) [22]. At a high specific energy input of 7 eV $molecule^{-1}$, the authors achieved conversions up to 57 % i.e., four times higher than the maximum of 15 % in the standard configuration. For the same conditions, the energy efficiency increased by a factor 10, reaching 20 % with the heat exchanger compared to 2 % in the standard design. Interestingly, the results with quenching at atmospheric pressure were close to the best results in the standard configuration at low pressure (200 mbar) but did not exceed the energy efficiency of about 30 %.

Most of the above results were obtained in MW plasmas, or otherwise in argon arc discharges with CO_2 addition. To the best of our knowledge, no previous research has studied an arc plasma reactor in pure CO_2 with nozzle and heat exchanger. In this work, we investigate for the first time the effect of quenching on the CO_2 conversion in an arc discharge with integration of either a nozzle or heat exchanger. Our arc plasma reactor exhibits a very flexible design, which permits a systematic study of how quenching can improve the CO_2 conversion in arc plasmas. Furthermore, we present a direct comparison with the best results for CO_2 conversion in MW discharges.

2. Methods

2.1 Experimental setup

The experimental setup is shown in **Figure 1**.

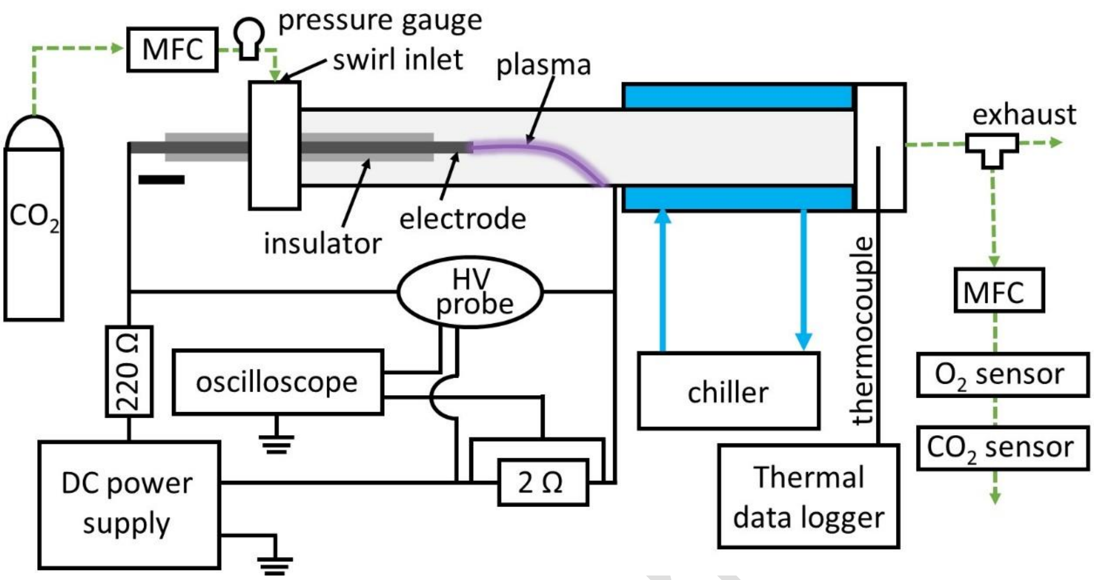

Figure 1 Schematic representation of the experimental setup for CO_2 conversion in an arc plasma reactor with quenching. The plasma is ignited between the high voltage electrode and the surrounding stainless-steel tube.

A cylinder with CO_2 gas (AirLiquide, purity 99.5 %) was connected to a mass flow controller (MFC, Bronkhorst El-Flow Select type F-201AV-50K) set to flow rates from 10 to 20 l_s/min (reference conditions 20 °C and 1 atm). The gas was inserted via four tangential inlets with a diameter of 1.5 mm, ensuring a forward swirling flow. The inlet pressure was monitored with a pressure gauge, to ensure that the pressure was the same for all the different designs (e.g., 0.45 barg at 15 l_s/min).

The plasma was generated between the stainless-steel pin electrode (0.8 cm diameter), surrounded by a Teflon insulator, and a grounded stainless-steel tube with 1.6 cm inner diameter and 2.0 cm outer diameter. Due to the grounded steel tube, the swirling flow was needed to stabilize the plasma and enable operation in a large current range. When the swirling flow is not used, like in our previous work with air plasma in a quartz tube and pin-to-pin configuration [23], the plasma could not be sustained in this case. The electrode distance, defined as the distance from the electrode tip to the start of the quenching zone, was varied between 5 and 11 cm. The quenching designs are described in more detail in **Section 2.2**. When water cooling is applied, the reactor is connected to a chiller (DZ5000LS-QX, Vevor) maintaining a water temperature of 20 °C.

The reactor was powered by a current-controlled power supply unit (PSU, Technix SR12KV-10kW) with negative polarity and a ballast resistor of 220 Ω. The current signal was determined by measuring the voltage drop across a 2 Ω shunt resistor, while the voltage was measured with a high voltage probe (Tektronix P6015A). These electrical signals were recorded with a two-channel oscilloscope (Keysight InfiniVision DSOX1102A 100 MHz). The input current was varied from 0.7 to 1 A, resulting in a plasma power between 300 and 1500 W, calculated from the product of the measured voltage and current.

At the outlet, the gas temperature is measured using K-type thermocouples at 55 cm from the gas inlet. The outlet gas after the reactor was sampled at 0.5 l_s/min with an MFC (Bronkhorst type F-200DV Low dP) and sent to an optical oxygen sensor (FDO2, Pyroscience) and an NDIR CO_2 sensor (FlowEvo, SmartGas GmbH).

The formulas to analyze the data are taken from our previous work [24]. Every experiment is repeated three times for statistical analysis, sometimes the error bars in the figures are too small to be visible. The error propagation with, e.g., the MFC measurement error, is included in the calculations.

The conversion is calculated with (eq.1):

$$\chi = \frac{1 - y_{CO_2}^{out}}{1 + \frac{y_{CO_2}^{out}}{2}} \quad \text{(eq.1)}$$

Where $y_{CO_2}^{out}$ is the output fraction of CO_2. This formula is valid since we only use CO_2 as an input gas. The specific energy input (SEI), is defined as:

$$\mathrm{SEI\ [eV\ molecule^{-1}]} = \frac{\mathrm{Plasma\ power\ [kW]}}{\mathrm{Flow\ rate\ [l_s\ min^{-1}\ ]}} \cdot \left(60\ \left[\frac{\mathrm{s}}{\mathrm{min}}\right] \cdot 24.1\ \left[\frac{\mathrm{l}}{\mathrm{mol}}\right] \cdot\ 6.24 \cdot 10^{21} \left[\frac{\mathrm{eV}}{\mathrm{kJ}}\right] \cdot \mathrm{N_A^{-1}} \left[\frac{\mathrm{mol}}{\mathrm{molecule}}\right]\right) \quad \text{(eq.2)}$$

And the resulting energy efficiency is defined as:

$$\eta\ [\%] = \frac{\chi_{\mathrm{CO_2}}[\%] \cdot \Delta \mathrm{H_R}°[\mathrm{eV\ molecule^{-1}}]}{\mathrm{SEI\ [eV\ molecule^{-1}]}} \quad \text{(eq.3)}$$

With $\Delta H_R°$ is 2.93 eV molecule^{-1}: the standard enthalpy of the dissociation reaction of CO_2. The energy efficiency is calculated based on the plasma power, which is most common in the context of plasma reactor design, and it allows to compare our data with results from literature. However, energy losses in the PSU or the cost of the cooling unit are not included. This would be important for calculating the real impact when integrating our technology in a full process, as discussed in more detail in **Section 3.8**.

2.2 Reactor designs for quenching

Thanks to the simple design of the arc reactor, consisting of a pin electrode surrounded by a grounded tube counter-electrode, various quenching methods can be easily studied. We tested five basic designs, as presented in **Figure 2**.

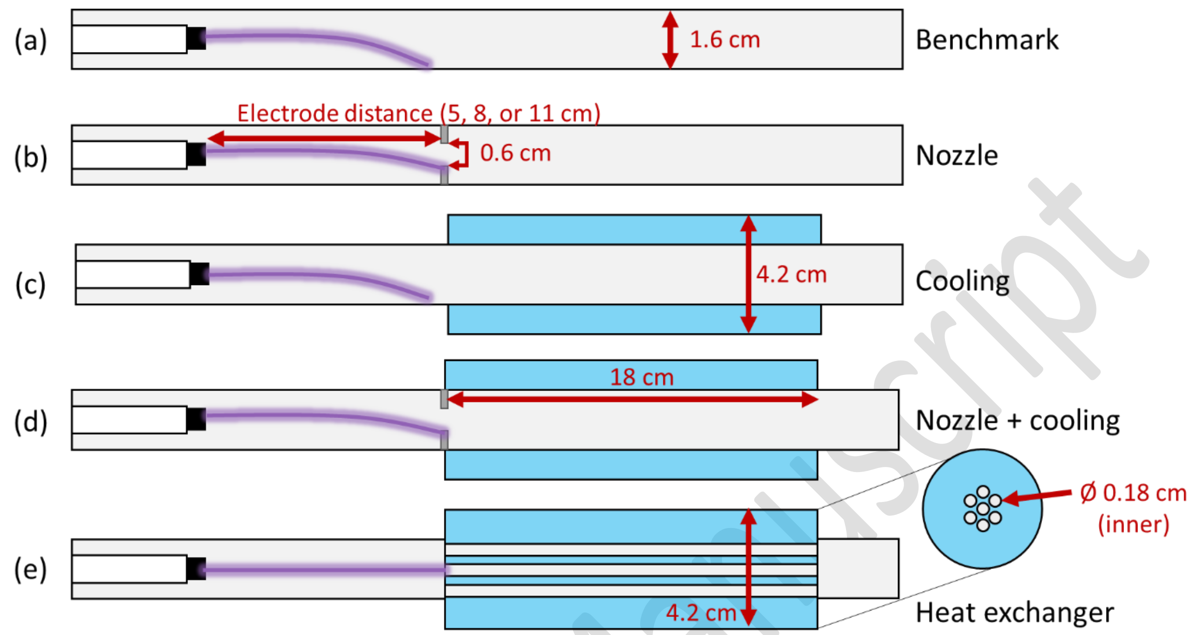

Figure 2 Cross sections of the different reactor designs to investigate quenching after a CO_2 arc plasma: (a) the benchmark, (b) nozzle, (c) double wall cooling, (d) combined nozzle and wall cooling, and (e) heat exchanger designs. The important dimensions are indicated in red; when not indicated, they are the same as in the other designs.

The benchmark (**Figure 2**a) is a straight, stainless-steel tube with an internal diameter of 1.6 cm. The electrode tip is at a distance of 8 to 15 cm from the swirl inlet and the total length until the outlet is 50 cm, similar for all designs. The nozzle (**Figure 2**b) is a round constriction with a diameter of 0.6 cm and a thickness of 1.5 cm. The cooling design (**Figure 2**c) consists of a double wall (with cooling water, connected to the chiller) with an outer diameter of 4.2 cm and a length of 18 cm. A combination of those two designs results in the nozzle + cooling design (**Figure 2**d). Finally, the heat exchanger (**Figure 2**e) is a basic version of the shell-and-tube heat exchanger principle. It consists of seven effluent channels with an outer diameter of 0.32 cm and an inner diameter of 0.18 cm (1/8-inch Swagelok stainless steel gas lines), enclosed in a tube with 4.2 cm outer diameter. The plasma and cooling tubes are connected through flanges.

Although the different designs involve various restrictions to the flow in the form of a nozzle, or the heat exchanger, the effects of these on the pressure inside the plasma are minimal, as we measured the same pressure in each case. For instance, the restriction caused by the heat exchanger is minimal, due to the large number of tubes used. While the area of the nozzle is 0.28 cm², the effective area of the heat exchanger is 0.18 cm². Hence, we can safely conclude that the differences observed for the different designs are not due to different pressures.

3. Results and discussion

First, we will compare the benchmark reactor with the nozzle in **Section 3.1**. We will then present the improved performance of the different cooling designs in **Section 3.2**, based on both the double wall and the heat exchanger, including a discussion of the arc dynamics in **Section 3.3**. The effect of the electrode distance is demonstrated in **Section 3.4**, followed by a discussion on the possible detrimental effects of cooling in **Section 3.5**. **Section 3.6** gives an overview of all designs in terms of conversion and energy efficiency, followed by a comparison between arc and MW designs in **Section 3.7**. Finally, we list some considerations regarding the realistic application of this technology in **Section 3.8**.

3.1 Effect of the nozzle

Figure 3 presents the CO_2 conversion at (a) different powers and (b) SEI values, for both the nozzle and the benchmark. The benchmark reactor clearly shows a lower conversion than the nozzle design. The energy efficiencies will be discussed in **Section 3.6**.

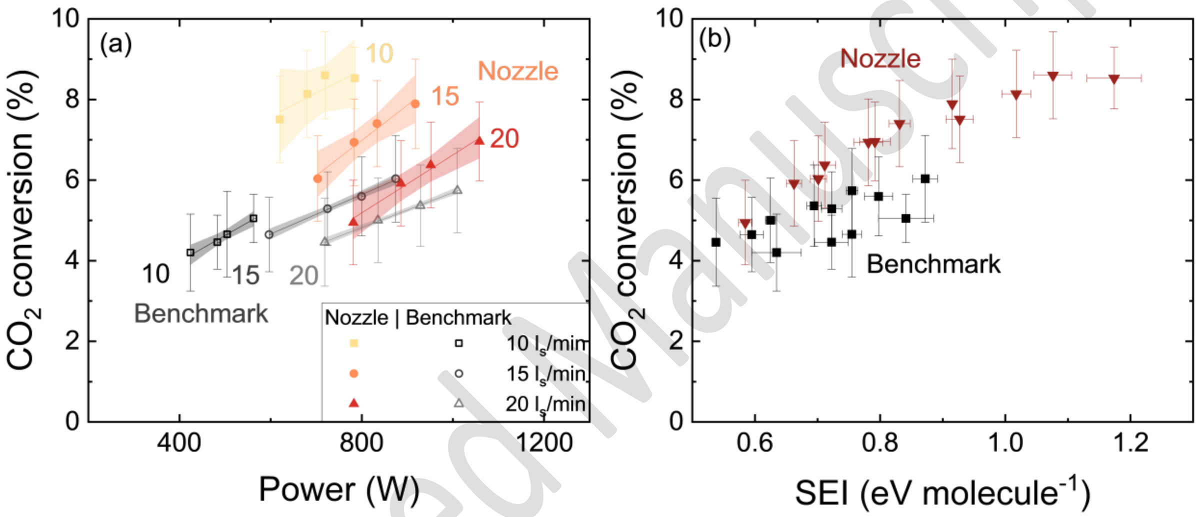

Figure 3 CO_2 conversion at (a) different powers, for three different flow rates (squares for 10 l_s/min, circles for 15 l_s/min, and triangles for 20 l_s/min) , with an indication of the 95 % confidence interval of the fit, and (b) different specific energy inputs (SEI), both for the benchmark (black squares) and nozzle (red triangles) with 11 cm electrode distance.

The results presented in **Figure 3**a are in line with our expectations: the conversion increases for lower flow rates (corresponding to longer residence times) and higher powers. At every flow rate, the subsequent points of increasing power correspond to an input current of 0.7, 0.8, 0.9 and 1 A, respectively. However, the benchmark cannot couple the same power to the plasma as the nozzle, even when the same conditions of input current and flow rate are applied. For example, at 10 l_s/min, the power in the benchmark is at maximum 600 W, while the nozzle is able to reach 800 W at this flow rate. This can be explained by the difference in plasma length between the two designs. In case of the benchmark, the average voltage is 0.6 kV for all input currents at 10 l_s/min. In the nozzle design, the plasma can elongate further, by attaching to the nozzle at the outlet and achieving higher voltage of 0.8 kV. With a higher voltage, a higher power and thus SEI (eq. 2) can be obtained. The arc dynamics will be discussed in more detail in the following sections.

The SEI range is much larger for the nozzle (from 0.6 to 1.2 eV molecule^{-1}) than for the benchmark (0.5 to 0.9 eV molecule^{-1}), as indicated in **Figure 3**b. The larger SEI corresponds to a higher conversion in the nozzle design, with a maximum of 8.6 %, compared to maximum 6 % in the benchmark. Considering conditions with a similar SEI, the nozzle still reaches a higher conversion. At 0.85 eV molecule^{-1} for example, it increases from 5.0 % to 7.4 %. This indicates that, besides the increase in power, due to the rise in plasma length, the nozzle has an additional effect on the performance.

This positive effect likely arises from the enhanced mixing after the plasma [15]. Indeed, the nozzle creates turbulence and enforces the hot core gas to mix with the cooler surrounding gas, providing faster cooling and limiting the recombination reactions (R1 and R2; cf. Introduction) in the effluent.

3.2 Comparing the different cooling designs

Figure 4 presents the CO_2 conversion as a function of SEI, for (a) cooling, (b) nozzle + cooling, and (c) heat exchanger. In (d), the outlet temperature is plotted as a function of time, to compare the cooling effect of the different designs.

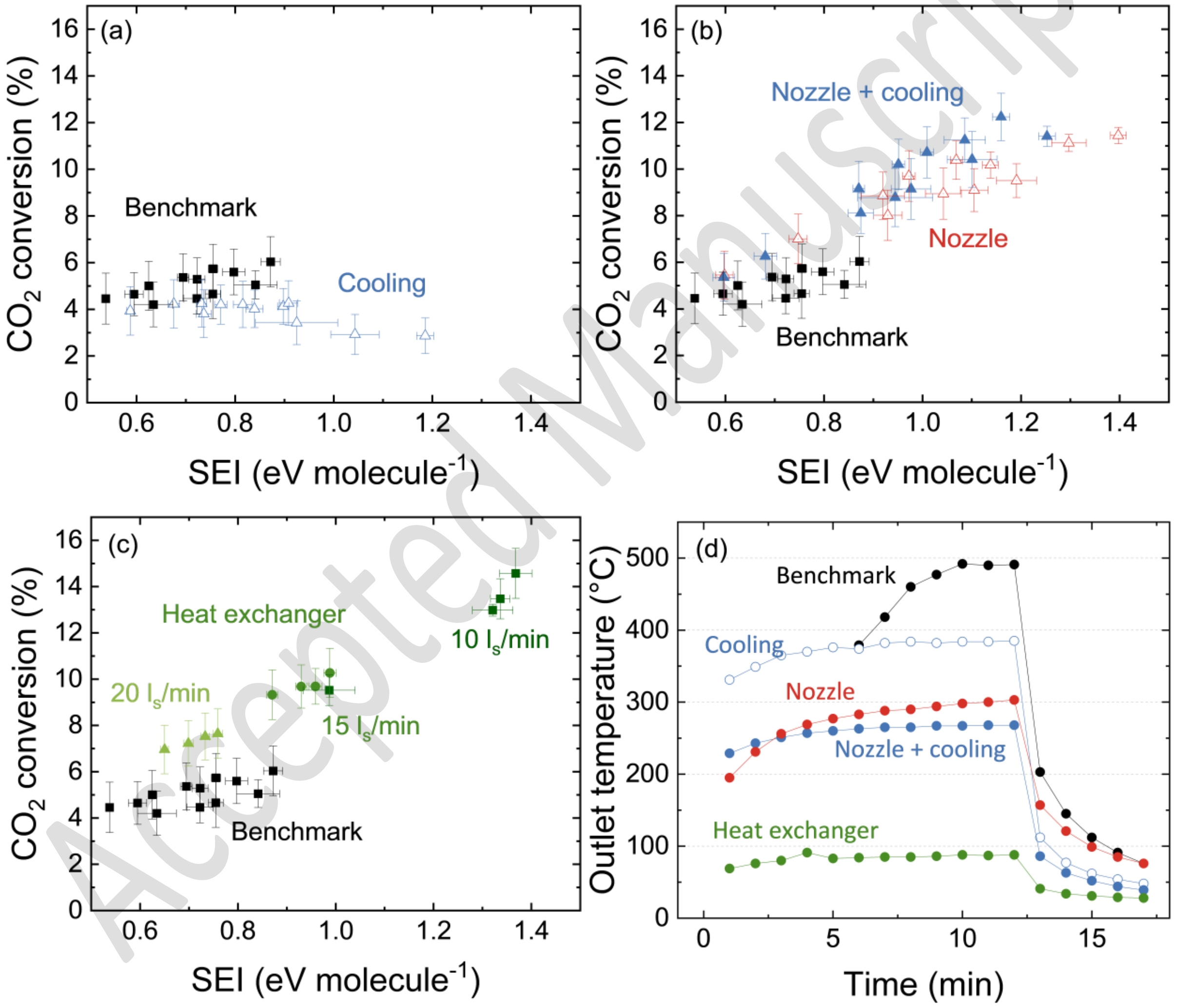

Figure 4 CO_2 conversion as a function of SEI, for (a) cooling design (open blue triangles) compared to the benchmark (black squares, (b) combined nozzle and cooling (blue triangles) compared to nozzle without cooling (open red triangles), and (c) heat exchanger (green triangles for 20 l_s/min, circles for 15 l_s/min, and squares for 10 l_s/min), all with an 8 cm electrode distance. In each case, the benchmark is also shown for comparison. (d) Outlet temperature as a function of time for the five different designs at 20 l_s/min and 1A. The power was turned off after 13 min. Note that the benchmark was operated for a shorter time, to limit the maximum temperature and protect reactor components. The measurement also started at time zero, but the first data point is shifted, so that the drop in temperature aligns with the other designs.

Applying (double wall) cooling appears detrimental for the conversion, as shown in **Figure 4**a. The conversion is lower than the benchmark at similar values of SEI and even decreases for higher SEI values. This indicates that the onset of cooling is too early, and quenching occurs before the maximum conversion is reached. This will be discussed further in **Section 3.5**. Note that a higher SEI can reached than the benchmark, even without an attachment point like a nozzle. This effect can be explained by the colder gas boundary layer, increasing the drag force and pushing the attachment point of the arc further downstream [25].

When the double wall cooling is added behind the nozzle, the conversion is clearly better than the benchmark, mainly due to the higher SEI values that can be reached, similar to **Figure 3**b. However, the conversion is not significantly better than the nozzle without cooling (**Figure 4**b), at least in this SEI range. The nozzle + cooling design reaches a maximum conversion of 12.2 %, compared to maximum 11 % in case of the nozzle without cooling. It thus seems that the gas mixing due to the nozzle provides more significant cooling than when the gas is in contact with the cold wall. Indeed, the nozzle has a clear benefit when compared to cooling (without nozzle) (**Figure 4**a). The nozzle likely helps to maintain the plasma within the reactor volume before cooling and provides the additional benefits of enhanced gas mixing and plasma elongation through attachment at the nozzle.

The cooling with heat exchanger is clearly the most beneficial. **Figure 4**c demonstrates a significantly higher conversion at the same SEI values as the benchmark, for example improving from 5.7 % to 7.6 % at 0.7 eV molecule^{-1}. Three regions can be distinguished for the heat exchanger, aligning with the three different flow rates. This can be explained by the stable plasma (see **Section 3.3**) resulting in a more constant power input, so that the flow rate has larger effect in resulting SEI values. The lowest flow rate yields the highest SEI, and because of the (roughly) linear correlation between SEI and conversion, the maximum conversion of 14.6 % is reached at the flow rate of 10 l_s/min, corresponding to an SEI of 1.4 eV molecule^{-1}.

The temperature at the outlet in **Figure 4**d gives an indication of the different cooling capacities of all designs. The outlet temperature in the benchmark case is as high as 500 °C. Introducing (double wall) cooling decreases the temperature to 385 °C, but a nozzle is more efficient and reduces the temperature to 300 °C without extra cooling, and to 270 °C in combination with cooling. This confirms that gas mixing after the nozzle provides a faster and more effective way of cooling than the double wall. Indeed, the improved gas mixing after the nozzle induces enough turbulence to improve the heat transfer to the walls and it increases the overall heat loss in the system, explaining why the results of the nozzles without and with extra cooling are so similar, as seen in **Figure 4**b. Finally, the heat exchanger causes even more efficient cooling, bringing the outlet temperature down to 90 °C. Even though the surface of the heat exchanger is smaller than for the double wall cooling (58 cm^2 compared to 75 cm^2), the surface to volume ratio of the heat exchanger is much larger (23 cm^{-1} compared to 2.5 cm^{-1}). In other words, the heat exchanger ensures a much better contact between the effluent gas and the cold wall, explaining the low outlet temperature and improved performance.

3.3 Electrical characteristics of different cooling designs

To explain the different performance of the various cooling designs, another factor to account for is the difference in SEI range between the designs. Why can the heat exchanger reach up to 1.4 eV molecule^{-1}, compared to only 0.9 eV molecule^{-1} in the benchmark? This can be explained by the plasma stability, demonstrated by the voltage and current signals, as displayed in **Figure 5** for (a) the benchmark and (b) the heat exchanger designs. These arc dynamics are well described for plasma torches [26].

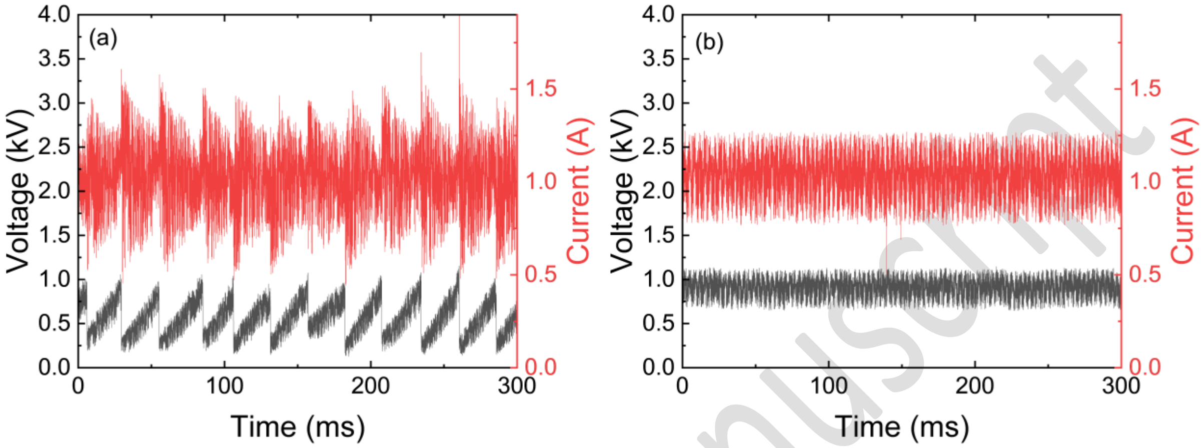

Figure 5 Temporal behavior of plasma voltage and current, for (a) the benchmark and (b) the heat exchanger with an electrode distance of 8 cm. Both designs operate at 10 l_s/min and 1 A input current.

In case of the benchmark, the plasma exhibits the characteristic restriking mode of a gliding arc, with periodic movement of the arc along the grounded electrode and typical voltage fluctuation (**Figure 5**a) [27]. In the heat exchanger, however, the plasma is more stable and characterized by the takeover arc regime (**Figure 5**b), probably due to a more stable attachment of the arc. In our reactor, the average voltage is significantly higher in the takeover mode (e.g., 0.9 kV) than in the restriking mode (e.g., 0.5 kV) as seen in **Figure 5**. This yields a larger power for the same input conditions, explaining the higher SEI values and thus also the higher conversion.

In summary, the combined effect of faster cooling and higher SEI range due to more stable plasma, enhances the performance, for both the nozzle and the heat exchanger, with the latter demonstrating superior performance.

3.4 Effect of electrode distance

Figure 6 illustrates the effect of the electrode distance on the CO_2 conversion as a function of the SEI, for (a) the heat exchanger and (c) the nozzle without cooling. The temporal variation of voltage is presented in (b) and (d) for the respective designs.

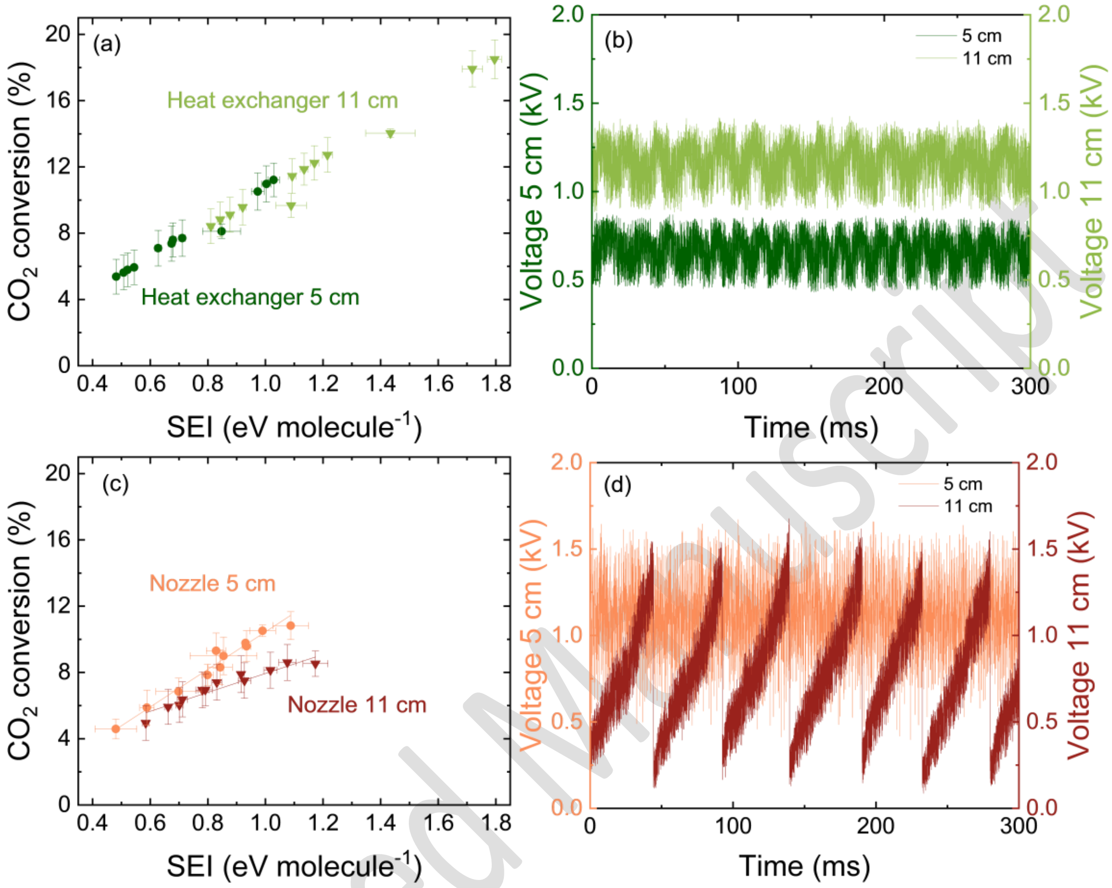

Figure 6 CO_2 conversion as a function of SEI, for two different electrode distance (circles for 5 cm, triangles for 11 cm), for (a) the heat exchanger and (c) the nozzle. Temporal behavior of the voltage for (b) the heat exchanger at conditions of maximum SEI, i.e. 10 l_s/min and 1A; and (d) the nozzle at conditions of similar SEI, i.e. 1.08 eV molecule^{-1}.

The electrode distance proves to be a determining parameter for the performance. A larger electrode distance is clearly beneficial in case of the heat exchanger (**Figure 6**a). The SEI range in the 5 cm case is maximum 1.1 eV molecule^{-1}, although the rising trend in conversion is evident. With a longer electrode distance of 11 cm, the SEI can reach up to 1.8 eV molecule^{-1} at the same conditions of 10 l_s/min and 1 A. This trend can again be attributed to the longer plasma length. The plasma can attach easily to the heat exchanger and form a stable channel. A longer electrode distance thus yields a longer plasma, resulting in a higher voltage, as shown in **Figure 6**b, hence, more power can be coupled. As a result, the heat exchanger with 11 cm electrode distance can achieve much higher conversion, i.e., at maximum 18.5 %.

However, a longer electrode distance is only beneficial when comparing similar plasma modes, as demonstrated by the results of the nozzle in **Figure 6**c. The results of the shorter distance (5 cm) are slightly better than for 11 cm at similar SEI values. The voltage signal in **Figure 6**d demonstrates a clear difference between both cases. At 5 cm, the plasma operates in the takeover mode, compared to the restriking mode in case of 11 cm. The nozzle is probably more difficult to attach than the heat exchanger, due to the higher velocity in the nozzle throat [14]. Probably, the arc keeps gliding somewhere in the tube when the distance is too great, resulting in a different operating mode at 11 cm than at 5 cm. Consequently, the afterglow is further away from the nozzle and quenching happens too late, so that the recombination reactions have taken place already, thus explaining the lower conversion. In summary, these results indicate that the performance can be optimized at the largest electrode distance that can maintain a stable plasma in the takeover mode.

3.5 Why does cooling not always help?

Figure 7 presents the results for the cooling design at electrode distances of 8 and 11 cm, illustrating (a) the CO_2 conversion as a function of SEI, and (b) the temporal voltage signal. The data at 8 cm is also shown in **Figure 4**a.

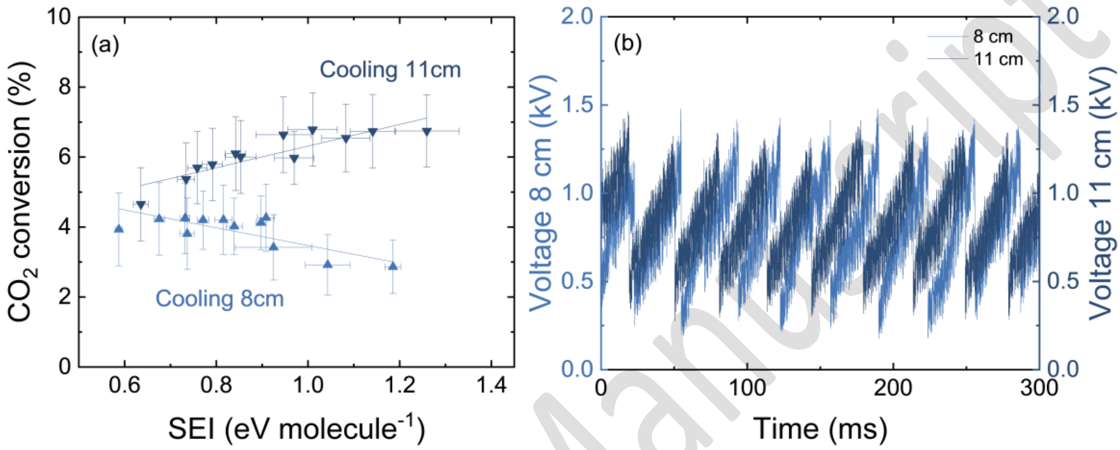

Figure 7 (a) CO_2 conversion as a function of SEI, and (b) temporal behavior of the plasma voltage for different electrode distances (up light-blue triangles for 8 cm, down dark-blue triangles for 11 cm) in the cooling design without nozzle.

Obviously, the design with double wall cooling displays opposite trends in conversion as a function of SEI for different electrode distances. The results at low SEI (~ 0.6 eV molecule^{-1}) are relatively close, with a conversion between 4 and 5 % (**Figure 7**a). The conversion increases with SEI in the case of 11 cm, as expected, but the opposite trend is observed for the 8 cm electrode distance. The conversion drops to values as low as 2.9 %, compared to 6.7 % conversion in the case of 11 cm. The difference in performance cannot be explained by a difference in the plasma operation mode, as both operate in the restriking mode (**Figure 7**b).

Instead, the observations in **Figure 7**a can be explained by the effect of quenching location. For a higher SEI input, the plasma extends freely and propagates into the double wall cooler. In case of a shorter electrode distance, the early onset of cooling is detrimental for the performance, because the conversion has not reached its maximum value yet. This is in line with a recent combined modelling and experimental study, where Ceulemans et al. [28] studied the balance between CO_2 splitting and recombination reactions and demonstrated that the latter only become dominant in the afterglow of a gliding arc plasma. In our cooling design with a longer electrode distance, the quenching only starts after the CO_2 conversion has reached its maximum, and thus it is beneficial for the performance. This negative trend for smaller electrode distances is not observed in the designs with a nozzle or heat exchanger, because they have physical borders that limit the plasma size. A model specific for these experiments can help to explain these trends in quenching location and will be part of future work. Overall, these results confirm that the cooling needs to happen only in the afterglow for an improved performance and not within the arc length for the range of SEI under study.

3.6 Overview of the performance for the different designs

Figure 8 compares the benchmark to three cooling designs in terms of (a) CO_2 conversion and (b) energy efficiency. The (double wall) cooling is not presented, because we demonstrated it typically exhibits lower performance.

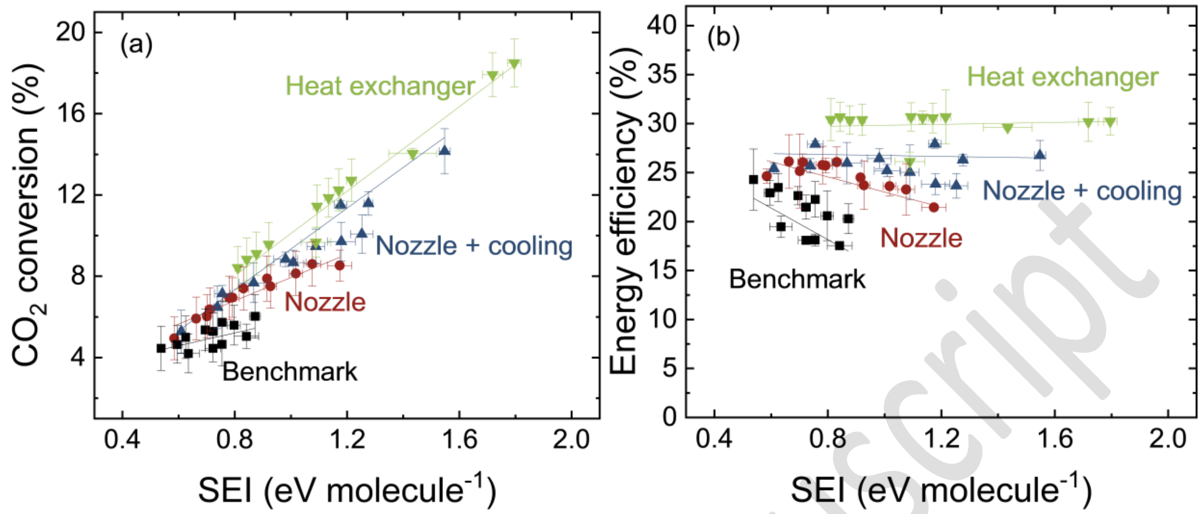

Figure 8 Overview of the results in terms of (a) CO_2 conversion and (b) energy efficiency as a function of SEI. Four designs are compared: the benchmark (black squares), nozzle without (red circles) and with cooling (blue up triangles), and heat exchanger (green down triangles). The electrode distance is 11 cm in all designs.

The enhanced CO_2 conversion is clearly demonstrated for all three cooling designs in **Figure 8**a. Any method of quenching will result in a higher conversion at the same SEI as the benchmark. More importantly, the quenching designs can change the plasma mode, due to the attachment of the arc to the nozzle or heat exchanger, thereby extending the plasma length. Hence, the resulting power in the plasma can be much higher, expanding the SEI range, even up to 1.8 eV molecule^{-1} for the heat exchanger operated at 10 l_s/min and 1 A, in the stable takeover mode. The CO_2 conversion increases linearly with SEI for all designs, but the results of the heat exchanger are consistently higher than for the other designs, indicating that it is the most effective way of cooling to prevent the recombination reactions.

The energy efficiency completes our understanding of the comparison between the cooling designs, and is displayed in **Figure 8**b. The benchmark shows the typical trend that a higher conversion at higher SEIs is accompanied by a drop in energy efficiency. This happens when the conversion rises to a lower extent than the SEI (cf. equation 3 in **Section 2.1**). The nozzle also shows a downward trend in efficiency, but it is still higher than the benchmark, e.g. at 0.8 eV molecule^{-1}, the energy efficiency increases from 20.6 % to 26.1 %. Adding a cooled double wall after the nozzle yields a slight improvement in conversion, but the effect on the energy efficiency is more significant, because the trend is less negative. Finally, the heat exchanger outperforms all other designs, with a constant energy efficiency of 30 % in the full SEI range.

From our experiments, it is difficult to separate whether specific plasma-chemical interactions or flow dynamics could also play a role. Overall, our experiments suggest that simply the difference in cooling efficiency is the most important, since the heat exchanger has an outlet temperature of less than 100 °C compared to about 250 °C in the designs with the nozzles and about 500 °C in the benchmark. A model specific for these experiments, as well as sophisticated laser diagnostics, can help to explain the observed trends and will be part of future work.

In summary, the heat exchanger yields a factor three enhancement in the CO_2 conversion, from maximum 6.0 % in the benchmark to 18.5 %, and at the same time, the energy efficiency also improves by a factor 1.5, from 20.5 % in the benchmark, to 30.2 %. This clearly demonstrates that the heat exchanger is the most effective cooling method in our study. Although it was previously believed that extremely high quenching rates are needed to preserve products from conversion [10], our study demonstrates that even a simple heat exchanger (hence, without much extra cost) could suffice to mitigate the issue with recombination reactions.

3.7 Comparison between arc and MW plasma for CO_2 conversion

Interestingly, our results are comparable to the MW results reported by Hecimovic et al. [22]. They were able to couple much higher powers in the plasma (up to 3 kW), corresponding to an SEI of maximum 7 eV molecule^{-1}, which explains why their conversion is significantly higher (up to 60 %). However, in the same SEI range up to 2 eV molecule^{-1} and at atmospheric pressure, our heat exchanger results align exactly with the results in the MW plasma, as the authors reported a conversion of about 16 % for an energy efficiency of 25 %.

Earlier works attributed the good performance of warm plasmas, such as (gliding) arc and MW plasmas, to specific plasma effects (e.g., electron impact reactions and vibrational-translational non-equilibrium) [6,11]. However, recent *in-situ* experiments in MW plasmas have demonstrated that the heavy particles in the plasma are in thermal equilibrium with the gas [29–31]. This means that both the conversion and energy efficiency have a theoretical limit that can be determined by thermodynamic equilibrium calculations, as explained by Bekerom et al. [29]. At low SEI, the conversion is limited when the available energy cannot dissociate all molecules. At high SEI, the efficiency is limited when the energy input exceeds the reaction enthalpy for complete dissociation. D'Isa et al. [31] measured a maximum energy efficiency of 30 % and a gas temperature of 6000 K, which agrees exactly with this thermal equilibrium efficiency limit.

In our experiments, we achieved the same maximum efficiency of 30 %. Furthermore, a similar gas temperature of 6000 K was measured in a pin reactor by Becarra et al. [32], indicating that the same effects of thermal equilibrium are dominant, independent of the different physics that govern the MW and arc plasma. This is quite striking, because the latter is heated by DC current, and the former by electromagnetic fields, but it illustrates that these underlying mechanisms do not significantly alter the performance. Indeed, under these conditions, the thermal chemistry is dominant, and quenching is therefore essential to maintain the high conversion from the hot plasma core in the effluent.

Our arc plasma can probably be further optimized to achieve the same high conversions as in the MW plasma, when operating at higher power (and thus, SEI), although the advantage of the latter remains that they operate without electrodes and thus avoid problems of electrode erosion. For both plasma reactors, however, the total efficiency of the system is essential when considering practical applications. As highlighted in a recent study by Kiefer et al. [33], the efficiency of MW power supplies (i.e., fraction of power delivered by the PSU that is effectively delivered to the plasma) is limited to the order of 70 % at 2.45 GHz [34], while arc power supplies typically have higher efficiency (order of 80-90%) [35]. Moreover, arc plasma reactors are easier to engineer, a significant advantage when considering that any technology for electrification of the chemical industry has to be coupled with heat integration. Until now, there are no studies showing heat recovery of the residual energy for CO_2 conversion through preheating the input gas. Furthermore, the residual heat could be used to activate the reverse Boudouard reaction in a post-plasma carbon bed [36,37], which can further enhance the conversion and energy efficiency.

In summary, our results show that with efficient quenching, the CO_2 conversion rises linearly with the SEI, resulting in better performance. As a result, we obtain a constant energy efficiency, which does not drop upon rising SEI. However, the maximum energy efficiency obtained in our work is 30 %, in line with the thermal efficiency reported in literature [8,12,31]. Therefore, in our future work, we plan to apply heat recovery, by using the heat removed with the heat exchanger to preheat the input gas, so that the applied power can all be used for the conversion and does not have to be (partly) used for gas heating. We expect that the overall energy efficiency of the system will in this way increase further, important for industrial application.

3.8 Considerations for realistic application

With basic design principles, we already demonstrated significant improved performance in our arc reactor. Of course, the simple setup leaves room for further improvement and some factors must be considered for a more realistic application.

First, both the materials and geometry of the heat exchanger could be improved based on the well-established heat exchanger technology in the chemical industry. The heat transfer could be improved by using specific copper and nickel alloys, or even ceramics instead of stainless steel, although there will be a trade-off between the increased material cost and improved performance [38]. The material must also be able to withstand high temperatures, especially at the arc attachment point (above 6000 K), since it is crucial that the quenching happens close to the plasma. For the geometry, the surface area could be increased, and extra strategies such as tape inserts or surface roughness [39] might further improve the performance. From a process point of view, the heat exchanger can also facilitate heat integration with other processes, which is up to now not investigated in plasma reactors.

Second, we should note that the energy efficiency here is calculated based on the plasma power. When optimizing the reactor and PSU for realistic application, the plug power is more important. In our experiments, we measured the plug power for the condition of the highest conversion, i.e., of 10 l_s/min and 1 A. While the plasma power was 1.16 kW, the plug power was 2.08 kW, hence the plasma accounted for 55 % of the total consumption. Accounting for the plug power in the SEI calculation, this means that the energy efficiency of 30 % (based on plasma power) would decrease to 18 %, when based on plug power. As mentioned in **Section 3.7**, the arc power supply can certainly be optimized for a fixed reactor configuration and plasma power. For example, as explored in previous work from our group [40,41], the ballast resistor could be removed if inductive elements are used or if the topology of the PSU changes so that the current limitation is provided by the transformer. In this case, the energy efficiency based on the plug power will be close to the plasma energy efficiency.

Another important factor is the long-term stability of the plasma reactor. Kiefer et al. demonstrated for a MW plasma reactor that the performance remains stable for at least 30 h [33]. Similar long-term stability is expected in our arc reactor, and preliminary tests of 6 h for another (gliding) arc reactor in our lab revealed a stable conversion and energy efficiency within 3 %, although the electrode erosion must be considered on even longer time scales. The stainless-steel pin cathode used in our experiments could be further improved with better materials (e.g. tungsten alloys or graphite) or protected by active cooling, i.e., strategies from commercial (larger scale) thermal plasma arc torch applications [42]. Furthermore, operating the plasma reactors in parallel [35] or at lower current and higher voltage will also significantly limit the erosion, as the latter is primarily determined by the current. Higher currents will be needed when upscaling, but this can be optimized depending on the cost of electrode erosion. On the other hand, thermal spray torches go up to 400 A, compared to only

1 A in our experiments, which demonstrates that there exist solutions to mitigate electrode erosion and reactor stability.

It is important to put our results in the context of other CO_2 conversion technologies. Plasma technology certainly has interesting advantages, as outlined in the Introduction and the extensive review by Snoeckx and Bogaerts [6]. However, a quantitative comparison is often challenging since the evaluation parameters are very different between the various technologies. Therefore, a discussion on the economic feasibility and environmental impact could provide a more relevant comparison. We recently performed a detailed techno-economic and sustainability analysis of a scaled-up plasma process for CO_2 conversion, based on a warm plasma setup with similar parameters as the experiments in this work, and we compared the metrics to electrolysis (i.e., a zero-gap type low-temperature electrolyser). Both the techno-economic [43] and sustainability [44] assessment revealed favourable results for the plasma process, thanks to the simple setup and cost-effective materials.

Specifically, the production cost of CO was estimated at $ 671 per tonne of CO, compared to $ 962 for electrolysis, which are both competitive compared to CO transported in gas cylinders (up to $ 3000 per tonne). The electricity costs had the most significant contribution for both technologies but are expected to decrease from renewable sources in the future. A sensitivity analysis also revealed an optimal scenario with low-cost feedstock and equipment, so that the CO production could fall below $ 500 per tonne of CO, which is more feasible in the plasma reactors thanks to their simpler design and absence of costly catalysts.

In terms of environmental impacts, the plasma demonstrates reductions in 7 of the 10 environmental impact categories evaluated, when compared to the equivalent conventional process of partial combustion with fossil fuels. The plasma process could also achieve 40 % energy savings compared to electrolysis. Furthermore, adding a recycling loop of unreacted CO_2 increases the material circularity indicator to above 0.8, which is 10 % higher than electrolysis. Finally, also the Green Chemistry metrics are more favourable than electrolysis by around 10 – 30 %. More details can be found in our previous work [43,44].

The upscaling of the arc plasma under study here will probably be slightly different from the case study of [43,44], which was based on many plasma reactors in parallel, while the arc plasma under study here should be upscaled towards industrial thermal plasma arc torch designs [42]. However, the characteristics of the process will be similar.

In future work, such comprehensive cost and sustainability studies will also be interesting to investigate for the arc plasma in this work. For example, the impact of the CO_2 source and possible purification costs, as well as heat integration are interesting subjects for such studies. Since our simple heat exchanger was already quite effective to enhance the performance, a passive cooling system with heat integration might be sufficient for improved performance, while avoiding the energy cost of the cooler. It should be noted that studies at such low technology readiness level are not applicable to specific cases for companies, but modelling such costs remains a valuable tool to identify the most relevant optimization strategies.

Overall, the findings in our study are a promising next step to improve carbon capture, utilization, and storage (CCUS) technologies for the electrified production of chemicals. The rapid reduction of CO_2 emission is crucial to limit climate change, and decarbonization will remain the priority. However, in the transition period, CCUS is essential as one of the key mitigation strategies to achieve net zero by 2050 [2]. Together with direct electrification, avoided demand and more renewable energy, improving CO_2 conversion by plasma technology can help to achieve our climate goals.

4 Conclusion

We performed a systematic investigation on the effect of various quenching methods on the CO_2 conversion and energy efficiency in an arc discharge. We demonstrate that post-plasma cooling can significantly enhance the performance by preventing the recombination reactions. Our results clearly show that a stainless-steel heat exchanger provides the most effective quenching. The conversion reaches up to 18 %, which is a factor three higher than the maximum of 6 % in the benchmark (without quenching). In addition, thanks to the linear correlation between conversion and SEI, the energy efficiency is constant upon rising SEI, reaching 30 %, a factor 1.5 higher than the maximum energy efficiency in the benchmark. Introducing a nozzle in the reactor after the plasma region, also improves the performance, even without wall cooling. The conversion then reaches 12 %, a factor two higher than the benchmark. These results follow the same trend as reported by Hecimovic et. al. [22], indicating that there is no fundamental difference in the underlying processes between a MW and arc discharge and that both are governed by the thermal efficiency.

Furthermore, our results show that a stable arc plasma provides better conversion and energy efficiency than when the arc is in an unstable regime. The unstable restriking mode is common for the benchmark design, without cooling options. Introducing a nozzle or heat exchanger provides an attachment point for the arc, which induces a transition from the restriking mode to the more stable takeover mode. Thanks to this stable arc elongation, the average voltage is higher, and more power can be coupled into the plasma, resulting in improved performance.

Interestingly, we show that cooling not always helps to improve the performance. We observe a drop in conversion by a factor of 2.3 for an 8 cm electrode distance when compared to the 11 cm distance, in the case of the double wall cooler without nozzle at SEI higher than 0.9 eV molecule^{-1}. This highlights the importance of the quenching location for improved performance, i.e., cooling should not happen within the arc length for the investigated SEI range, but in the afterglow, after the maximum conversion is reached, and recombination reactions become dominant over the CO_2 splitting reactions. A model specific for these experiments, as well as sophisticated laser diagnostics can help to explain the observed trends and will be part of future work.

Finally, we outlined some considerations for a more realistic application of this technology. The basic design of the heat exchanger already gives promising results, but the geometry and material choice can certainly be optimized. Strategies to mitigate electrode erosion, as well as long term stability tests, and a more comprehensive energy cost analysis with heat integration are other important steps that will be part of future work.

5 Acknowledgments

We acknowledge financial support from the Fund for Scientific Research (FWO) Flanders (Grant ID 110221N) and the European Research Council (ERC) under the European Union's Horizon 2020 research and innovation program (grant agreement No 810182 - SCOPE ERC Synergy project).

6 References

[1] K. Calvin, D. Dasgupta, G. Krinner, et al., IPCC, 2023: Climate Change 2023: Synthesis Report. Contribution of Working Groups I, II and III to the Sixth Assessment Report of the Intergovernmental Panel on Climate Change. IPCC, Geneva, Switzerland., Intergovernmental Panel on Climate Change (IPCC), 2023. https://doi.org/10.59327/IPCC/AR6-9789291691647.

[2] IEA, Net Zero Roadmap: A Global Pathway to Keep the 1.5 °C Goal in Reach, Paris, 2023. https://www.iea.org/reports/net-zero-roadmap-a-global-pathway-to-keep-the-15-0c-goal-in-reach (accessed January 24, 2024).

[3] A. Bogaerts, G. Centi, Plasma Technology for CO2 Conversion: A Personal Perspective on Prospects and Gaps, Front Energy Res 8 (2020). https://doi.org/10.3389/fenrg.2020.00111.

[4] I. Tsonev, C. O'Modhrain, A. Bogaerts, Y. Gorbanev, Nitrogen Fixation by an Arc Plasma at Elevated Pressure to Increase the Energy Efficiency and Production Rate of NOx, ACS Sustain Chem Eng 11 (2023) 1888–1897. https://doi.org/10.1021/acssuschemeng.2c06357.

[5] A. Bogaerts, E.C. Neyts, Plasma Technology: An Emerging Technology for Energy Storage, ACS Energy Lett 3 (2018) 1013–1027. https://doi.org/10.1021/acsenergylett.8b00184.

[6] R. Snoeckx, A. Bogaerts, Plasma technology - a novel solution for CO2 conversion?, Chem Soc Rev 46 (2017) 5805–5863. https://doi.org/10.1039/c6cs00066e.

[7] A. Fridman, S. Nester, L.A. Kennedy, A. Saveliev, O. Mutaf-Yardimci, Gliding arc gas discharge, Prog Energy Combust Sci 25 (1999) 211–231. https://doi.org/10.1016/S0360-1285(98)00021-5.

[8] R. Vertongen, A. Bogaerts, How important is reactor design for CO2 conversion in warm plasmas?, Journal of CO2 Utilization 72 (2023) 102510. https://doi.org/10.1016/J.JCOU.2023.102510.

[9] I. V. Bilera, Yu.A. Lebedev, Plasma-Chemical Production of Acetylene from Hydrocarbons: History and Current Status (A Review), Petroleum Chemistry 62 (2022) 329–351. https://doi.org/10.1134/S0965544122010145.

[10] V. Vermeiren, A. Bogaerts, Plasma-Based CO2 Conversion: To Quench or Not to Quench?, The Journal of Physical Chemistry C 124 (2020) 18401–18415. https://doi.org/10.1021/acs.jpcc.0c04257.

[11] A. Fridman, Plasma chemistry, Cambridge university press, 2008.

[12] V.D. Rusanov, A.A. Fridman, G. V Sholin, The physics of a chemically active plasma with nonequilibrium vibrational excitation of molecules, Soviet Physics Uspekhi 24 (1981) 447–474. https://doi.org/10.1070/PU1981v024n06ABEH004884.

[13] N. V. Chekmarev, D.A. Mansfeld, A. V. Vodopyanov, S. V. Sintsov, E.I. Preobrazhensky, M.A. Remez, Enhancement of CO2 conversion by counterflow gas quenching of the post-discharge region in microwave plasma sustained by gyrotron radiation, Journal of CO2 Utilization 82 (2024) 102759. https://doi.org/10.1016/J.JCOU.2024.102759.

[14] S. Van Alphen, A. Hecimovic, C.K. Kiefer, U. Fantz, R. Snyders, A. Bogaerts, Modelling post-plasma quenching nozzles for improving the performance of CO2 microwave plasmas, Chemical Engineering Journal 462 (2023) 142217. https://doi.org/10.1016/j.cej.2023.142217.

[15] A. Hecimovic, F.A. D’Isa, E. Carbone, U. Fantz, Enhancement of CO2 conversion in microwave plasmas using a nozzle in the effluent, Journal of CO2 Utilization 57 (2022) 101870. https://doi.org/10.1016/j.jcou.2021.101870.

[16] E.R. Mercer, S. Van Alphen, C.F.A.M. van Deursen, T.W.H. Righart, W.A. Bongers, R. Snyders, A. Bogaerts, M.C.M. van de Sanden, F.J.J. Peeters, Post-plasma quenching to improve conversion and energy efficiency in a CO2 microwave plasma, Fuel 334 (2023) 126734. https://doi.org/10.1016/j.fuel.2022.126734.

[17] J. Li, X. Zhang, J. Shen, T. Ran, P. Chen, Y. Yin, Dissociation of CO2 by thermal plasma with contracting nozzle quenching, Journal of CO2 Utilization 21 (2017) 72–76. https://doi.org/10.1016/j.jcou.2017.04.003.

[18] W. Bongers, H. Bouwmeester, B. Wolf, F. Peeters, S. Welzel, D. van den Bekerom, N. den Harder, A. Goede, M. Graswinckel, P.W. Groen, Plasma-driven dissociation of CO2 for fuel synthesis, Plasma Processes and Polymers 14 (2017) 1600126. https://doi.org/10.1002/ppap.201600126.

[19] H. Sekiguchi, A. Kanzawa, T. Honda, Thermal quenching effects on plasma synthesis of NO and plasma decomposition of CO2, Plasma Chemistry and Plasma Processing 9 (1989) 257–275. https://doi.org/10.1007/BF01054285.

[20] H. Kim, S. Song, C.P. Tom, F. Xie, Carbon dioxide conversion in an atmospheric pressure microwave plasma reactor: Improving efficiencies by enhancing afterglow quenching, Journal of CO2 Utilization 37 (2020) 240–247. https://doi.org/10.1016/j.jcou.2019.12.011.

[21] A. Huczko, A. Szymański, Thermal decomposition of carbon dioxide in an argon plasma jet, Plasma Chemistry and Plasma Processing 4 (1984) 59–72. https://doi.org/10.1007/BF00567372.

[22] A. Hecimovic, C.K. Kiefer, A. Meindl, R. Antunes, U. Fantz, Fast gas quenching of microwave plasma effluent for enhanced CO2 conversion, Journal of CO2 Utilization 71 (2023) 102473. https://doi.org/10.1016/J.JCOU.2023.102473.

[23] I. Tsonev, H. Ahmadi Eshtehardi, M.-P. Delplancke, A. Bogaerts, Importance of geometric effects in scaling up energy-efficient plasma-based nitrogen fixation, Sustain Energy Fuels 8 (2024) 2191–2209. https://doi.org/10.1039/D3SE01615C.

[24] B. Wanten, R. Vertongen, R. De Meyer, A. Bogaerts, Plasma-based CO2 conversion: How to correctly analyze the performance?, Journal of Energy Chemistry 86 (2023) 180–196. https://doi.org/10.1016/j.jechem.2023.07.005.

[25] E. Noguès, P. Fauchais, M. Vardelle, P. Granger, Relation Between the Arc-Root Fluctuations, the Cold Boundary Layer Thickness and the Particle Thermal Treatment, Journal of Thermal Spray Technology 16 (2007) 919–926. https://doi.org/10.1007/s11666-007-9120-x.

[26] J.P. Trelles, E. Pfender, J. Heberlein, Multiscale Finite Element Modeling of Arc Dynamics in a DC Plasma Torch, Plasma Chemistry and Plasma Processing 26 (2006) 557–575. https://doi.org/10.1007/s11090-006-9023-5.

[27] J.F. Coudert, M.P. Planche, P. Fauchais, Characterization of d.c. plasma torch voltage fluctuations, Plasma Chemistry and Plasma Processing 16 (1995) S211–S227. https://doi.org/10.1007/BF01512636.

[28] K. Wang, S. Ceulemans, H. Zhang, I. Tsonev, Y. Zhang, Y. Long, M. Fang, X. Li, J. Yan, A. Bogaerts, Inhibiting recombination to improve the performance of plasma-based CO2 conversion, Chemical Engineering Journal 481 (2024) 148684. https://doi.org/10.1016/j.cej.2024.148684.

[29] D.C.M. van den Bekerom, J.M.P. Linares, T. Verreycken, E.M. van Veldhuizen, S. Nijdam, G. Berden, W.A. Bongers, M.C.M. van de Sanden, G.J. van Rooij, The importance of thermal dissociation in CO2 microwave discharges investigated by power pulsing and rotational Raman scattering, Plasma Sources Sci Technol 28 (2019) 55015. https://doi.org/10.1088/1361-6595/aaf519.

[30] G.J. van Rooij, D.C.M. van den Bekerom, N. den Harder, T. Minea, G. Berden, W.A. Bongers, R. Engeln, M.F. Graswinckel, E. Zoethout, M.C.M. van de Sanden, Taming microwave plasma to beat thermodynamics in CO2 dissociation, Faraday Discuss 183 (2015) 233–248. https://doi.org/10.1039/C5FD00045A.

[31] F.A. D'Isa, E.A.D. Carbone, A. Hecimovic, U. Fantz, Performance analysis of a 2.45 GHz microwave plasma torch for CO2 decomposition in gas swirl configuration, Plasma Sources Sci Technol 29 (2020) 105009. https://doi.org/10.1088/1361-6595/abaa84.

[32] M. Becerra, J. Nilsson, S. Franke, C. Breitkopf, P. André, Spectral and electric diagnostics of low-current arc plasmas in CO2 with N2 and H2O admixtures, J Phys D Appl Phys 57 (2024) 015202. https://doi.org/10.1088/1361-6463/acfcc6.

[33] C.K. Kiefer, R. Antunes, A. Hecimovic, A. Meindl, U. Fantz, CO2 dissociation using a lab-scale microwave plasma torch: An experimental study in view of industrial application, Chemical Engineering Journal 481 (2024) 148326. https://doi.org/10.1016/J.CEJ.2023.148326.

[34] H. Zhu, Y. Huang, S. Yin, W. Zhang, Microwave plasma setups for CO2 conversion: A mini-review, Green Energy and Resources 2 (2024) 100061. https://doi.org/10.1016/j.gerr.2024.100061.

[35] C. O'Modhrain, G. Trenchev, Y. Gorbanev, A. Bogaerts, Upscaling Plasma-Based CO2 Conversion: Case Study of a Multi-Reactor Gliding Arc Plasmatron, ACS Engineering Au (2024). https://doi.org/10.1021/acsengineeringau.3c00067.

[36] F. Girard-Sahun, O. Biondo, G. Trenchev, G.J. van Rooij, A. Bogaerts, Carbon bed post-plasma to enhance the CO2 conversion and remove O2 from the product stream, Chemical Engineering Journal 442 (2022) 136268. https://doi.org/10.1016/j.cej.2022.136268.

[37] Z. Li, T. Yang, S. Yuan, Y. Yin, E.J. Devid, Q. Huang, D. Auerbach, A.W. Kleyn, Boudouard reaction driven by thermal plasma for efficient CO2 conversion and energy storage, Journal of Energy Chemistry 45 (2020) 128–134. https://doi.org/10.1016/j.jechem.2019.10.007.

[38] S. Mahmoudinezhad, M. Sadi, H. Ghiasirad, A. Arabkoohsar, A comprehensive review on the current technologies and recent developments in high-temperature heat exchangers, Renewable and Sustainable Energy Reviews 183 (2023) 113467. https://doi.org/10.1016/j.rser.2023.113467.

[39] S.A. Marzouk, M.M. Abou Al-Sood, E.M.S. El-Said, M.M. Younes, M.K. El-Fakharany, A comprehensive review of methods of heat transfer enhancement in shell and tube heat exchangers, J Therm Anal Calorim 148 (2023) 7539–7578. https://doi.org/10.1007/s10973-023-12265-3.

[40] V. Ivanov, T. Paunska, S. Lazarova, A. Bogaerts, S. Kolev, Gliding arc/glow discharge for CO2 conversion: Comparing the performance of different discharge configurations, Journal of CO2 Utilization 67 (2023) 102300. https://doi.org/10.1016/j.jcou.2022.102300.

[41] F. Manaigo, O. Samadi Bahnamiri, A. Chatterjee, A. Panepinto, A. Krumpmann, M. Michiels, A. Bogaerts, R. Snyders, Electrical Stability and Performance of a Nitrogen–Oxygen Atmospheric Pressure Gliding Arc Plasma, ACS Sustain Chem Eng 12 (2024) 5211–5219. https://doi.org/10.1021/acssuschemeng.3c08257.

[42] M.I. Boulos, P.L. Fauchais, E. Pfender, Handbook of Thermal Plasmas, Springer International Publishing, Cham, 2023. https://doi.org/10.1007/978-3-030-84936-8.

[43] J. Osorio-Tejada, M. Escriba-Gelonch, R. Vertongen, A. Bogaerts, V. Hessel, CO2 conversion to CO via plasma and electrolysis: a techno-economic and energy cost analysis, Energy Environ Sci 17 (2024) 5833–5853. https://doi.org/10.1039/D4EE00164H.

[44] M. Escribà-Gelonch, J. Osorio-Tejada, R. Vertongen, A. Bogaerts, V. Hessel, Sustainability assessment of plasma-based and electrolytic CO2 conversion to CO, J Clean Prod 488 (2025) 144578. https://doi.org/10.1016/j.jclepro.2024.144578.